

# Effect of Atmosphere Change Paths on the Induced Chemical Expansion

O. VALENTIN<sup>1\*</sup>, E. BLOND<sup>1</sup>, A. JULIAN<sup>2</sup>, N. RICHET<sup>3</sup>

<sup>1</sup> Institut PRISME EA 4229, University of Orléans, Polytech'Orléans, 8 rue L. de Vinci, 45072 Orléans, France

<sup>2</sup> SPCTS - UMR 6638 - CNRS, 47 avenue Albert Thomas, 87065 Limoges, France

<sup>3</sup> Air Liquide CRCD, 1 chemin Porte des Loges BP126, 78354 Jouy en Josas, France

\*e-mail: olivier.valentin@univ-orleans.fr

---

## Abstract

This study presents the relevant aspects of the approach developed at Institut PRISME to model strain in the mixed ionic and electronic conductors (MIEC) membrane for reforming of methane into synthesis gas ( $H_2/CO$ ). This macroscopic approach is based on the assumption of strain partition and on the choice of oxygen activity as a state variable. It leads to a thermo-chemo-mechanical model taking into account oxygen diffusion as well as elastic, thermal and chemical expansion phenomena. A chemical expansion model is proposed. The kinetics of a macroscopic bulk diffusion model has been fitted by simulation to chemical dilatometry tests. The transient and the steady-state stress distribution in a membrane reactor for partial oxidation of methane (POM) have been simulated in various conditions.

**Keywords:** Mixed conductors, Membrane, Chemical expansion model, Oxygen vacancy

## WPLYW SPOSOBU ZMIANY ATMOSFERY NA WYWOŁYWANĄ EKSPANSJĘ CHEMICZNĄ

Niniejsze praca przedstawia stosowne aspekty podejścia do modelowania odkształcenia w membranie z mieszanych przewodników jonowo-elektronowych (MIEC) dla reformingu metanu w procesie syntezy gazu ( $H_2/CO$ ), rozwiniętego w Instytucie PRISME. To makroskopowe podejście opiera się na założeniu o podziale odkształcenia i na wyborze aktywności tlenu jako parametru stanu. Prowadzi to do termo-chemo-mechanicznego modelu biorącego pod uwagę dyfuzję tlenu, a także zjawiska ekspansji sprężystej, cieplnej i chemicznej. Zaproponowano model rozszerzalności chemicznej. Kinetyka w makroskopowym modelu dyfuzji objętościowej została dopasowana za pomocą symulacji do testów chemicznej dylatometrii. Rozkład naprężeń w stanie nieustalonym i ustalonym w reaktorze membranowym do częściowego utleniania metanu (POM) został zasymulowany w różnych warunkach.

**Słowa kluczowe:** przewodnik mieszane, membrana, model rozszerzalności chemicznej, wakancja tlenowa

---

## 1. Introduction

Dense mixed ionic and electronic conducting membranes (MIEC) have potential applications for partial oxidation of methane (POM) into synthesis gases ( $CO/H_2$ ) from the extraction of oxygen from air. The oxygen transport driving force is ensured by the gradient of oxygen chemical potential. The diffusion of the oxygen ions induces changes in valence and oxygen vacancy concentration variations, which lead to a macroscopic strain [1-3]. The same phenomenon is observed in other applications of non-stoichiometric oxide such as Solid Oxide Fuel Cells (SOFC) [4, 5]. In the POM process, the oxygen activity through the membrane may vary from oxidizing atmosphere (air) to reducing atmosphere ( $CH_4$ ) in a range of more than 20 orders of magnitude. In service, according to the boundaries conditions, it leads to strain-stress between the oxidizing side and the reducing side. At the membrane reactor scale these chemo-mechanical stresses affect the mechanical reliability of the whole structure [6]. From our knowledge, a few authors have proposed

mechanical stresses prediction in MIEC membranes. Yakabe [4] for SOFC, proposed a numerical simulation model to analyse in steady-state the chemical and thermal expansion in an inter-connector. Atkinson and Hendriksen [1, 7] have explored the relationship between operating conditions and membrane geometry and resulting stresses in the oxygen membrane separation.

This work focuses on the influence of operating conditions on the membrane stress field. In the first part the modelling of the chemical expansion is presented. The computational methods are then briefly described. In the next part, the identification method of kinetics is presented. The last part concerns various loading cases of simulations of a membrane.

## 2. Thermo-chemo-mechanical model

The chemical expansion is the strain which results from a change in composition of the material at the constant phase. These changes can be due to atmosphere and/or temperature variations. The chemically-induced strain does

not modify the elastic mechanical behaviour but comes in addition to the usual thermal expansion [8].

Assuming small strains, the total strain tensor is described by the symmetric part of the displacement gradient with respect to the spatial position. Then, the partition of deformations leads to write the total strain as the sum of all possible strains:

$$\varepsilon = \varepsilon_t + \varepsilon_e + \varepsilon_c, \quad (1)$$

where  $\varepsilon_t$  is the thermal strain tensor,  $\varepsilon_e$  is the elastic strain tensor and  $\varepsilon_c$  the chemical strain tensor. In the rest of the paper, bold symbols will refer to vector/tensor variables and regular ones will refer to scalar parameters.

The thermal strain tensor depends on temperature variation in a reversible way:

$$\varepsilon_t = \alpha \cdot (T - T_0) \cdot I, \quad (2)$$

where  $\alpha$  is the secant coefficient of linear thermal expansion,  $T_0$  a reference temperature and  $I$  the second rank identity tensor. Thermal deformation corresponds here exclusively to the deformation induced by temperature variation at constant composition and without any phase change.

Assuming the material is homogeneous and isotropic with linear thermal-elastic behaviour, the elastic strain is:

$$\varepsilon_e = \frac{1+\nu}{E} \cdot \sigma - \frac{\nu}{E} Tr(\sigma) \cdot I, \quad (3)$$

where  $\nu$  is Poisson's ratio,  $E$  Young's modulus,  $\sigma$  the stress tensor,  $I$  the second rank identity tensor and  $Tr(\sigma)$  is the trace of tensor  $\sigma$ .

The coefficient of thermal expansion was measured by dilatometry ( $\alpha_{20-900} = 1.1 \cdot 10^{-5} \text{ } ^\circ\text{C}^{-1}$ ). Young's modulus (125 GPa at 20°C, 95 GPa at 900°C) has been measured by the ultrasonic method [9]. The tensile strength (120 MPa) and Weibull's modulus (2.9) have been obtained using four point bending tests on an MTS-2/M testing machine with a load sensor of 10 kN. Other data like Poisson's ratio (0.25), thermal conductivity ( $2 \text{ W}\cdot\text{m}^{-1}\cdot^\circ\text{C}^{-1}$ ) or specific heat ( $500 \text{ J}\cdot\text{g}^{-1}\cdot^\circ\text{C}^{-1}$ ) have been chosen from literature values for such ceramics.

### 3. Chemical expansion model

The literature reports strains coming from the variation in concentration of a substance in the material [10]. These strains are stress-free according to the approach of Larché *et al.* [11]. In order to model the thermo-chemo-mechanical behaviour of such ceramics, the majority of phenomenological works proposed a linear relation between chemical expansion and oxygen vacancy concentration [12-15].

The chemical expansion model proposed hereafter is an improvement of the previous studies [16, 17]. In these models, it has been chosen to directly link chemical expansion to oxygen activity. The main assumption of the proposed approach is the reversible dependence on chemical strain tensor with oxygen activity variation. Furthermore, because this work focuses on atmosphere effects on mechanical stress, temperature influence in relation to chemical expansion is neglected. Therefore, at macroscopic scale, assuming isotropic chemical strain, three parameters are necessary to describe the dependence on chemical strain in relation to

oxygen activity:

$$\varepsilon_c = \begin{cases} \beta \cdot \ln\left(\frac{a}{a_{ref}}\right) & \text{for } a > a_{min} \\ \beta \cdot \ln\left(\frac{a_{min}}{a_{ref}}\right) = \varepsilon_c^{max} & \text{for } a \leq a_{min} \end{cases} \quad (4)$$

where  $\varepsilon_c$  is the linear chemical induced strain,  $\beta$  is a dimensionless coefficient of chemical expansion ( $-1.78 \cdot 10^{-4}$ ),  $a_{ref}$  is the zero chemical strain oxygen activity reference (air for our material),  $a$  is the actual oxygen activity at the considered point and  $a_{min}$  is the minimal oxygen activity under which chemical expansion is constant ( $3 \cdot 10^{-5}$ ).

Fig. 1 shows the chemical expansion model fitted with both results of dilatometry and X-ray measurements for  $\text{La}_{0.8}\text{Sr}_{0.2}\text{Fe}_{0.7}\text{Ga}_{0.3}\text{O}_{3-\delta}$  perovskite-type material.  $\text{La}_{1-x}\text{Sr}_x\text{Fe}_{1-y}\text{Ti}_y\text{O}_{3-\delta}$  material previously studied [17] follows a similar behaviour and could be described with the same model.

The chemical expansion is linear with logarithm of  $p\text{O}_2$  in the range from  $3 \cdot 10^{-5}$  atm to 1 atm. From  $3 \cdot 10^{-5}$  atm to  $10^{-21}$  atm the chemical expansion appears constant.

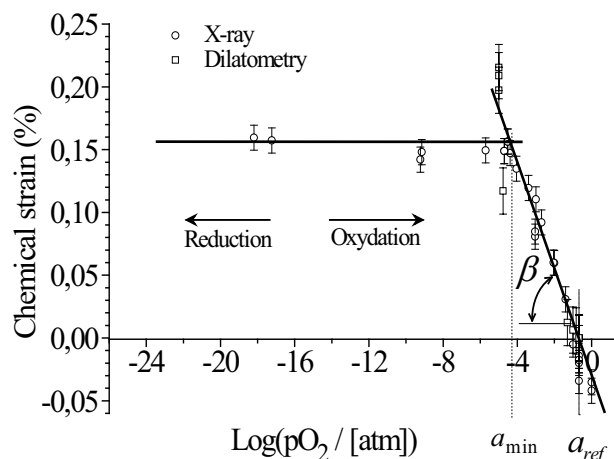


Fig. 1. Chemical expansion vs. oxygen activity, results by X-ray and dilatometry for  $\text{La}_{0.8}\text{Sr}_{0.2}\text{Fe}_{0.7}\text{Ga}_{0.3}\text{O}_{3-\delta}$ .

### 4. Oxygen transport model

The oxygen diffusion can be represented using the simplified Wagner's law:

$$J = D_0 \cdot \exp\left(\frac{-Q}{R \cdot T}\right) \cdot \text{grad}(\ddot{u} \ a)), \quad (5)$$

where  $J$  is the oxygen flux,  $a$  the oxygen activity,  $D_0$  the "intrinsic" oxygen diffusivity,  $Q$  the activation energy and  $R$  the ideal gas constant.

The time scale of permeation gets longer as the temperature is reduced. At low temperature ( $< 500^\circ\text{C}$ ), the diffusion process is stopped because of the Arrhenius term in Eq. (5). Consequently, oxygen activity in the material does not evolve and neither does chemical expansion. Surface exchanges are not considered in this study. This is still a work in progress which will be presented in future papers.

## 5. Computational method

The chemical strain behaviour proposed above has been implemented in Abaqus finite elements software using the UMAT procedure. For the oxygen transfer computation a macroscopic modelling of oxygen permeation through the membrane according to Eq. (5) has been implemented in UMAT procedure.

The geometries of the cylindrical sample for dilatometry and tubular membrane of CMR have been modelled in 2D with axisymmetric elements. Oxygen activity is directly applied on boundaries. Computations are realized in three steps: heat transfer computation to obtain the temperature field; oxygen transfer computation, using temperature field to obtain the oxygen activity field; thermo-mechanical simulation, including the dedicated strain behaviour, the temperature gradient and the oxygen activity distribution. Numerical tests were performed to ensure that the solutions were independent of the mesh size.

## 6. Identification of permeation kinetics

To identify the parameters of Eq. (5), the simulation of an expansion test on a cylindrical sample (6.7 mm diameter and 5 mm long) under  $N_2$  and Air has been computed. The kinetics of heat transfers is assumed so much faster than oxygen permeation, that it is not the limiting step. Therefore, since the chemical expansion behaviour is known, the rate at which the sample exhibits its chemically-induced expansion expresses the kinetics of permeation. When permeation starts (depending on temperature) the chemical expansion occurs and a chemical strain adds thermal strain on the expansion curves.

The prescribed conditions for the simulation of expansion tests are detailed in Fig. 2. The boundary conditions of oxygen activity are applied along the contour of the geometry:  $10^{-5}$  for reducing and 0.21 for oxidizing. The homogeneous temperature field is imposed at a constant heating and cooling rate of  $2^\circ\text{C}/\text{min}$ . Classical mechanical boundary conditions are used to prevent rigid body displacements.

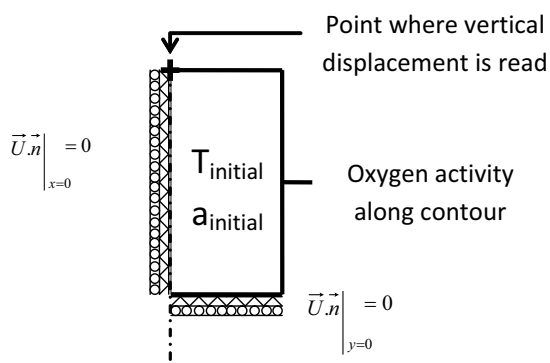


Fig. 2. Prescribed field and boundary conditions for the expansion test simulation.

The material is in equilibrium with air (initial state air) at the beginning of the reduction test, whereas the material is in equilibrium with nitrogen for the oxidizing one (initial state  $N_2$ ). More details about the dilatometry test are given in [17]. Fig. 3 for reducing and Fig. 4 for oxidizing step show how

the simulations match experiments with  $D_0 = 100 \text{ m}^2 \cdot \text{s}^{-1}$  and  $Q = 138 \text{ kJ}$ . These coefficients correspond to typical value of diffusivity equal to  $7.1 \cdot 10^{-5} \text{ m}^2 \cdot \text{s}^{-1}$  at  $900^\circ\text{C}$ .

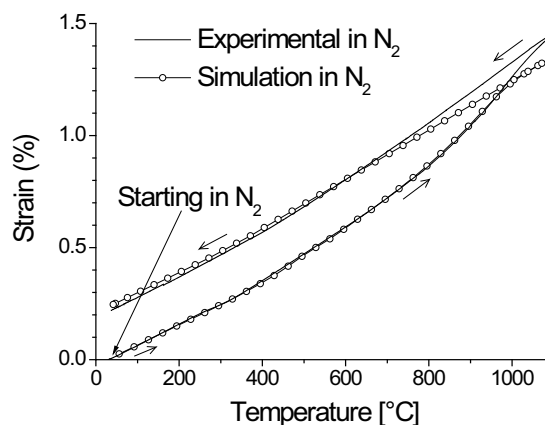


Fig. 3. Dilatometric curves in reduction, experimental vs. simulation, initial state is air.

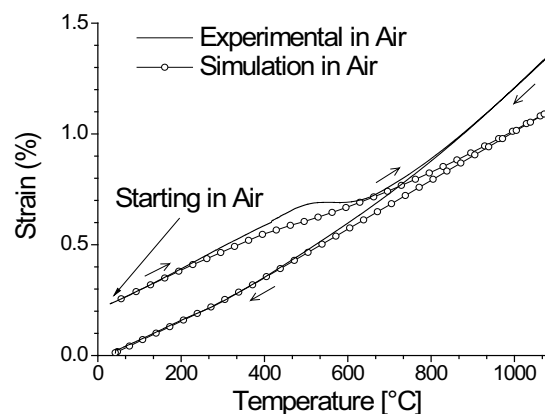


Fig. 4. Dilatometric curves in oxidation, experimental vs. simulation, initial state is  $N_2$ .

For the oxidizing test the deviation above  $500^\circ\text{C}$  should be attributed to the thermal sensitivity of chemical expansion.

It is significant to notice that the kinetic parameters are refined on the whole two tests, without distinction of oxidation and reduction stage. The simulation stays in agreement with the experiment but the results suggest that thermal activation of permeation differs between oxidation and reduction. The oxidizing kinetics should be faster than reduction.

However, the shape of the chemical expansion behaviour (logarithm) as demonstrated in [17] biases the perception of permeation kinetics when considering the dilatometric curves. Furthermore, the kinetics of diffusion and the oxygen surface exchange represent probably one of the most complex aspects in MIEC. Adler [18] said that a consensus had not yet emerged regarding the mechanisms and rate laws governing oxygen exchange with the bulk at the gas-exposed surface. It is necessary to refine further the kinetics to describe the tests correctly. The works are still in progress on a specific oxygen surface exchange law.

## 7. Simulations of a membrane

The thermo-chemo-mechanical simulations have been realized on a tubular membrane section of a 7.2 mm inner diameter, 1 mm thick. More information about the geometry

of the reactor is presented in [16]. The prescribed conditions for the membrane simulation are detailed in Fig. 5. The constant and homogeneous temperature field is fixed at 900°C in the structure.

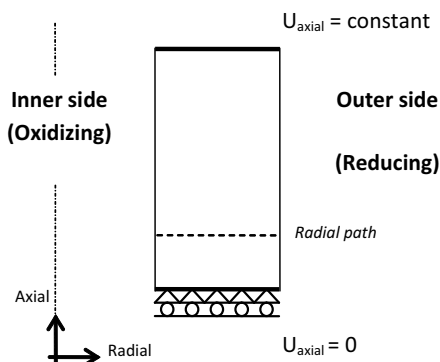


Fig. 5. Prescribed field and boundary conditions for the simulation of the tubular membrane section.

In this study of the atmosphere change path effect, the reference steady-state conditions chosen are  $a_{ref}$  on the inner side and  $a_{min}$  on the outer one. In fact, it corresponds to air and  $N_2$  respectively for the characterized material here.

All the results of stresses distributions presented hereafter are plotted following the radial path in section of membrane (Fig. 5). The stress distributions have been normalized to unity with respect to the maximum tensile stress reached during the reference steady-state conditions (axial stress on inner side). Tensile stresses are conventionally positive and compressive stresses negative.

When reaching the reference steady-state, the oxygen activity gradient through the thickness gives rise to chemical stresses. The steady-state stress distribution is plotted in Fig. 6. This straightforward approach has been presented by Atkinson [1] in an analytical approach. It corresponds exactly to the typical case of a cylinder heated on the outer side. If the atmosphere is reducing, the strain is positive and the stress is in compression. Vice versa, if the atmosphere is oxidizing, the strain is negative and the stress is in tension.

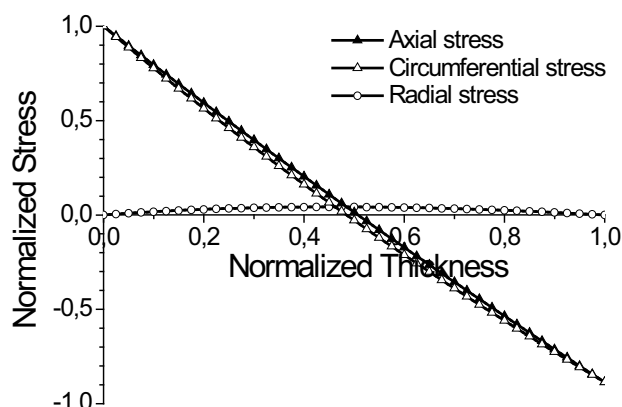


Fig. 6. Stresses due to chemical strain in membrane in steady-state.

In the reference steady-state, axial and circumferential stresses are almost the same. The inside surface of the membrane (oxidizing) is in tension and the outside in compression (reducing). In ceramic material tensile stresses are dangerous especially when they occur on surface. Therefore,

the inner side is mechanically critical in this situation. Radial stress is negligible.

When harder conditions are applied on the reducing side ( $< a_{min}$ ), the stress distribution in membrane is different because chemical expansion under  $a_{min}$  is constant. This is plotted in Fig. 7. In the steady state, the level of tensile stress on oxidizing side is 1.55 time higher than the level reached in the reference steady state. In highly reducing atmosphere, even if chemical expansion is constant above  $a_{min}$ , it leads to a worse situation in terms of mechanical reliability.

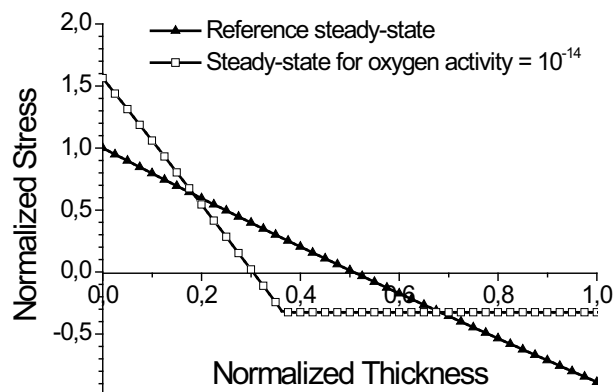


Fig. 7. Stress distribution due to chemical strain for oxygen activity reducing conditions under  $a_{min}$  ( $10^{-14}$ ).

## 8. Transient states

The transient state during a start-up is studied. The initial state for the membrane is sintering in air; it means that the oxygen activity is equal to 0.21 in the whole membrane. At the initial time, oxygen activity 0.21 is prescribed on the inner surface and  $1 \cdot 10^{-5}$  on the outer.

Transient stresses due to chemical strain in membrane during start-up from initial state air to the reference steady-state are shown in Fig. 8.

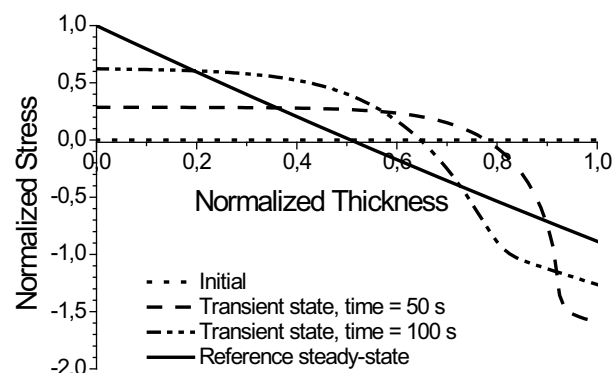


Fig. 8. Transient axial stresses due to chemical strain in membrane during start-up from initial state air to reference steady-state.

During start-up, there is tension of the inner side and compression of the outer side. Tensile stress on the inner surface increases from 0 to the stress of service. On the outer side compressive stress reaches 1.6 times steady state compressive stress. Such levels are not especially damaging for ceramic materials because compressive strength is considered at least ten times as high as tensile strength.

## 9. Conclusions

A thermo-chemo-mechanical model has been proposed. It has been used to quantify mechanical stress in steady and transient states. The level of tensile stresses reached during the steady-state is relatively high regarding the value of tensile strength and its Weibull's modulus. The calculation shows that the starting from initial state in equilibrium with air causes chemical shock with relatively high compressive stresses. The approach provides an indication of risks associated with atmosphere changes. This numerical tool can help to develop a strategy to optimize reactor management.

## Acknowledgements

The authors would like to express their gratefulness to E. Véron for X-ray measurement and I. Ben Chaabanne for help in English. The authors acknowledge Air Liquid and the ADEME for supporting this research.

## References

- [1] Atkinson A., Ramos T. M. G. M.: „Chemically-induced stress in ceramic oxygen ion-conducting membranes”, *Solid State Ionics*, 129, (2000), 259-269.
- [2] Miyoshi S., Hong J.-O., Yashiro K., Kaimai A., Nigara Y., Kawamura K., Kawada T., Mizusaki J.: „Lattice expansion upon reduction of perovskite-type  $\text{LaMnO}_3$  with oxygen-deficit nonstoichiometry”, *Solid State Ionics*, 161, (2003), 209-217.
- [3] Kharton V. V., Yaremchenko A. A., Patrakeeve M. V., Naumovich E. N., Marques F. M. B.: „Thermal and chemical induced expansion of  $\text{La}_{0.3}\text{Sr}_{0.7}(\text{Fe,Ga})\text{O}_{3-\delta}$  ceramics”, *J. Eur. Ceram. Soc.*, 23, (2003), 1417-1426.
- [4] Yakabe H., Yasuda I.: “Model Analysis of the expansion behavior of  $\text{LaCrO}_{3-\delta}$  interconnector under solid oxide fuel cell operation”, *J. Electrochem. Soc.*, 150, (2003), A35-A45.
- [5] Fu Q.X., Tietz F., Lersch P., Stover D.: „Evaluation of Sr- and Mn-substituted  $\text{LaAlO}_{3-\delta}$  as potential SOFC anode materials”, *Solid State Ionics*, 177, (2006), 1059-1069.
- [6] Pei S., Kleefisch M.S., Kobylinski T.P., Faber J., Uudovich C.A., Zhang-McCoy V., Dabrowski B., Balachandran U., Mieville R. L., Poeppel R.B.: „Failure mechanisms of ceramic membrane reactors in partial oxidation of methane to synthesis gas”, *Catal. Lett.*, 30, (1995), 201-212.
- [7] Hendriksen P. V., Larsen P. H., Mogensen M., Poulsen F. W., Wiik K.: “Prospects and problems of dense oxygen permeable membranes”, *Catal. Today*, 56, (2000), 283-295.
- [8] Adler S. B.: „Chemical expansivity of electrochemical ceramics”, *J. Am. Ceram. Soc.*, 84, (2001), 2117-2119.
- [9] Julian A., Juste E., Geffroy P.M., Tessier-Doyen N., Del Gallo P., Richet N., Chartier T.: „Thermal behaviour of  $\text{La}_{0.8}\text{Sr}_{0.2}\text{Fe}_{1-x}\text{Ga}_x\text{O}_{3-\delta}$  ( $x = 0$  or  $x = 0.3$ )”, *J. Eur. Ceram. Soc.*, 29, (2009), 2603-2610.
- [10] Krishnamurthy R., Sheldon B. W.: „Stresses due to oxygen potential gradients in non-stoichiometric oxides”, *Acta Mater.*, 52, (2004), 1807-1822.
- [11] Larché F. C., Cahn J. W.: „Overview no. 41 the interactions of composition and stress in crystalline solids”, *Acta Metall.*, 33, (1985), 331-357.
- [12] Larsen P. H., Hendriksen P. V., Mogensen M.: „Dimensional stability and defect chemistry of doped lanthanum chromites”, *J. Thermal Anal. Calor.*, 49, (1997), 1263-1275.
- [13] Boroomand F., Wessel E., Bausinger H., Hilpert K.: „Correlation between defect chemistry and expansion during reduction of doped  $\text{LaCrO}_3$  interconnects for SOFCs”, *Solid State Ionics*, 129, (2000), 251-258.
- [14] Hilpert K., Steinbrech R. W., Boroomand F., Wessel E., Meschke F., Zuev A., Teller O., Nickel H., Singheiser L.: „Defect formation and mechanical stability of perovskites based on  $\text{LaCrO}_3$  for solid oxide fuel cells (SOFC)”, *J. Eur. Ceram. Soc.*, 23, (2003), 3009-3020.
- [15] Li Y., Maxey Evan R., Richardson Jr J. W., Ma B., Lee T. H., Song S.-J.: „Oxygen non-stoichiometry and thermal-chemical expansion of  $\text{Ce}_{0.8}\text{Y}_{0.2}\text{O}_{1.9-\delta}$  electrolytes by neutron diffraction”, *J. Am. Ceram. Soc.*, 90, (2007), 1208-1214.
- [16] Blond E., Richet N.: „Thermomechanical modelisation of ion-conducting membrane for oxygen separation”, *J. Eur. Ceram. Soc.*, 28, (2008), 793-801.
- [17] Valentin O., Blond E., Julian A., Richet N.: „Loading path effect on the chemical expansion in substoichiometric LSF based perovskite”, *Comp. Mater. Sci.*, 46, (2009), 912-920.
- [18] Adler S. B., Chen X.Y., Wilsona J.R.: „Mechanisms and rate laws for oxygen exchange on mixed-conducting oxide surfaces”, *J. Catal.*, 245, (2007), 91-109.



Received 31 March 2010; accepted 5 May 2010